Identification of Motion Platform Using the Signal Compression Method with Pre-Processor and Its Application to Siding Mode Control

Min Kyu Park
Graduate School of Intelligent Mechanical Engineering, Pusan National University, Pusan 609-735, Korea
Min Cheol Lee*
School of Mechanical Engineering, Pusan National University, Pusan 609-735, Korea

In case of a single input single output (SISO) system with a nonlinear term, a signal compression method is useful to identify a system because the equivalent impulse response of linear part from the system can be extracted by the method. However even though the signal compression method is useful to estimate uncertain parameters of the system, the method cannot be directly applied to a unique system with hysteresis characteristics because it cannot estimate all of the two different dynamic properties according to its motion direction. This paper proposes a signal compression method with a pre-processor to identify a unique system with two different dynamics according to its motion direction. The pre-processor plays a role of separating expansion and retraction properties from the system with hysteresis characteristics. For evaluating performance of the proposed approach, a simulation to estimate the assumed unknown parameters for an arbitrary known model is carried out. A motion platform with several single-rod cylinders is a representative unique system with two different dynamics, because each single-rod cylinder has expansion and retraction dynamic properties according to its motion direction. The nominal constant parameters of the motion platform are experimentally identified by using the proposed method. As its application, the identified parameters are applied to a design of a sliding mode controller for the simulator.

Key Words : Identification, Motion Platform, Single Rod Cylinder, Expansion and Retraction Dynamic Properties, Signal Compression Method, Sliding Mode Control

1. Introduction

A single-rod cylinder has been widely used as an actuator of 6-DOF parallel motion platform reappearing a vehicle or an airplane motion because it is longer in stroke and smaller in size than a double-rod cylinder. The structure of a motion platform generally consists of a 6-DOF parallel manipulator, which is called Stewart platform (Stewart 1966). The platform is a closed loop form. It provides better load-to-weight ratio and rigidity than a serial manipulator. However, it is difficult to analyze dynamic properties of a motion platform because of non-linearity of its actuators caused by a difference of a volume according to each chamber. Many other researches for the identification of linear system have been carried out by using a least square method, an adaptive filter, and so on (Widrow and Stearns 1985 ; Masui et. al., 2000 ; Zou and Chan 1999). However, it is hard to apply these methods

* Corresponding Author,
E-mail : mclee@hyowon.pusan.ac.kr
TEL : +82-51-510-2439; **FAX** : +82-51-512-9835
Professor, School of Mechanical Engineering, Pusan National University, Pusan 609-735, Korea. (Manuscript **Received** December 5, 2001; **Revised** August 1, 2002)

to a nonlinear system, because these algorithms were based on a linear system (Lee and Aoshima 1989). In case of a single input single output (SISO) system with a nonlinear term, a signal compression method is useful to identify a system because the equivalent impulse response of linear part from the system can be extracted by the method (Lee and Aoshima 1989; Yang et. al., 1998). However even though the signal compression method is useful to estimate uncertain parameters of the system, the method cannot be directly applied to a unique system with hysteresis characteristics because it cannot estimate all of the two different dynamic properties according to its motion direction. Therefore, it is also difficult the signal compression method to identify a system with hysteresis characteristics such as a motion platform with several single-rod cylinders because each single-rod cylinder includes expansion and retraction dynamic properties according to its motion direction.

This paper proposes the signal compression method with a pre-processor to identify the system with hysterisis dynamics. The pre-processor plays a role of separating expansion and retraction properties from a system with hysteresis characteristics. To evaluate the proposed method, computer simulation for estimating parameters of the known system is carried out by using the proposed method. Identification of the 6-DOF parallel motion platform is experimentally carried out. As its application, a sliding mode controller is designed on the basis of the identified model of the platform. Sliding mode control algorithm is very effectively used for a nonlinear system, because this is robust against parameters and load variations (Lee et. al., 1998; Slotine 1985; Hashimoto et. al., 1987). The performance of the designed sliding mode controller is experimentally evaluated.

2. Signal Compression Method

2.1 Signal compression method

An ideal impulse signal for identifying a system has flat power spectrum in a wide frequency range. However, it is difficult to apply an impulse signal to real system because the magnitude of the signal is infinite and the period is very short. To solve these problem, an equivalent impulse signal is generated by using the signal compression method. The equivalent impulse has a flat power spectrum in a desired frequency range (Lee and Aoshima 1989). The equivalent impulse signal is transformed by the Fourier transform. After the signal in frequency domain passes through a mathematical phase-shift filter, the signal has a constant power and phase delay. If this signal in the frequency domain is transformed into the time domain through the inverse Fourier transform, the transformed signal called as test signal have a low amplitude and is lasted for a long time, as shown in Fig. 1 (Lee and Aoshima 1989; Yang et. al., 1998). Therefore, the test signal is able to be applied to a real system in order to estimate uncertain parameters. A response obtained by supplying the signal to the system is compressed through fast Fourier transform (FFT), inverse phase-shift filter, and inverse fast Fourier transform (IFFT). In this compression process, equivalent impulse response for a linear element can be indirectly obtained, because of being able to separate a linear element from the system with a nonlinear element. These processes are known as a signal compression method (SCM). Figure 2 is a general schematic diagram of the signal compression method (Lee and Aoshima 1989; Yang et. al., 1998).

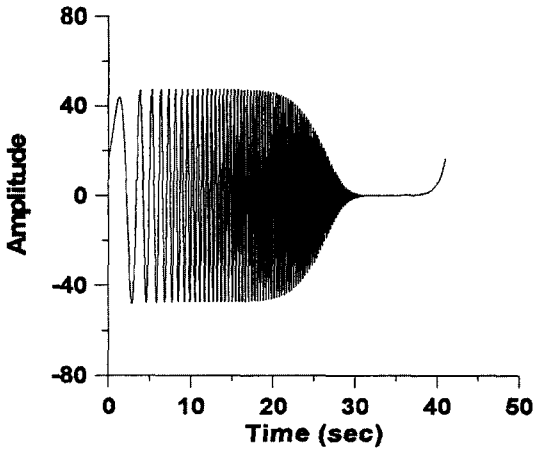

Fig. 1 Test signal

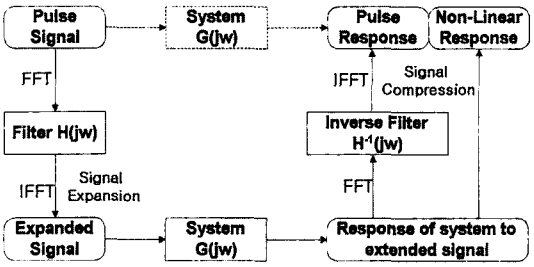

Fig. 2 Block diagram of signal compression method

2.2 Signal compression method with pre-processor

The signal compression method cannot be directly applied to a unique system with hysteresis characteristics because the dynamic models of expansion and retraction motion are different. Therefore, in case of this system, each dynamic model of the system must be obtained respectively. Therefore, this paper proposes the signal compression method with pre-processor able to separate each dynamics from two different dynamics. This method appends pre-processor to the signal compression method. The main function of the pre-processor is to separate expansion and retraction properties from a unique system. Increasing and decreasing parts of the test signal will cause the expansion motion and the retraction motion in the system, respectively. Therefore, the expansion and the retraction element can be separated by the sign of the derivative value of output signal. The sign of the derivative value for the expansion element is positive. The sign of that for the retraction element is negative.

Figure 3 shows the flow of the signal compression method with pre-processor. First, the impulse signal is transformed into the test signal of the SCM through the Fourier transform, the mathematical phase shift filter, and the inverse Fourier transform. The test signal is used as the reference trajectories which is applied to a unique system with two different dynamics according to its motion direction. The output signal of the system is measured by using sensor as shown in [Step 3] of Fig. 3. This signal shows that the expansion properties of the system are different from the retraction properties. Second, for separating the expansion elements and the retraction

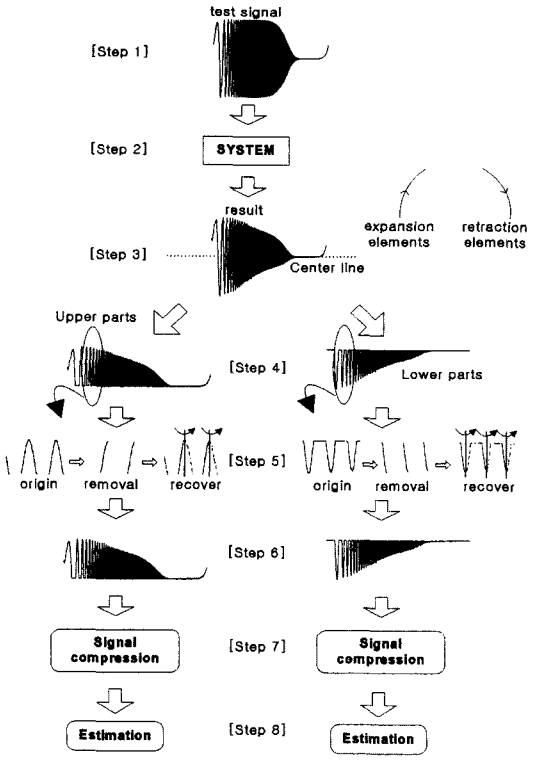

Fig. 3 Flow of the signal compression method with pre-processor

elements from the output signal, the datum line is necessary. Therefore, a center line of the output signal is used as the datum line. The signal is separated into upper and lower part from the center line as shown in [Step 4] of Fig. 3. Both the expansion elements and the retraction elements exist in upper parts as shown in origin process of [Step 5]. For getting the dynamic properties of the expansion elements, the retraction elements should be removed in upper parts to extract only the expansion elements as shown in removal process of [Step 5]. The signal generated by this process is discontinuous because of the removed parts. Therefore, for overcoming discontinuous signal, the removed parts can be recovered by folding signal of expansion elements on the basis of vertical symmetric axis. This process is shown as recover process of [Step5] of Fig. 3. The signal recovered by this process is not retraction elements of the system. This has the same properties as the opposite sides of the

expansion elements. In the lower parts, the same method is applied, this process is called the pre-processor. This method is applied to the whole range of upper parts and lower parts, respectively. After this procedure, the expansion dynamic elements only exist in the upper parts and the retraction dynamic elements only exist in the lower parts. Third, the equivalent impulse responses for a unique system with expansion and retraction dynamics are obtained by the signal compression process. By using the obtained equivalent impulse response, the unknown parameters of the linear part can be estimated. By comparing Bode plot of the transfer function of a model with that obtained from the equivalent impulse response of linear components, a natural frequency and a damping coefficient are estimated. Then, for better estimation, the cross-correlation between the impulse response of an assumed model and the equivalent impulse response obtained from a real system is used. The uncertain parameters such as natural frequency and damping coefficient of 2nd order system are continuously renewed when the obtained impulse response is closest to the impulse response from the assumed model. Finally the uncertain parameters are estimated when the cross-correlation is biggest.

The system which includes two different dynamic properties according to its motion direction can be identified by this procedure.

2.3 Evaluation in simulation

To evaluate the performance of the proposed method, a simulation to estimate the assumed parameters for an arbitrary known model is carried out.

The dynamic properties related to the expansion and retraction of model 1 are set to same values. The properties of model 2 and model 3 are set to different values, respectively. The selected models are listed in Table 1. Figures 4~10 show the estimation results for model 3. Figure 4 is the output signal from the model 3 when the test signal is supplied to the model. Each dynamics for the expansion and retraction motion is separated by the pre-processor as shown in [step 5] of Fig. 3. The separated signals are transformed into the equivalent impulse response by using the

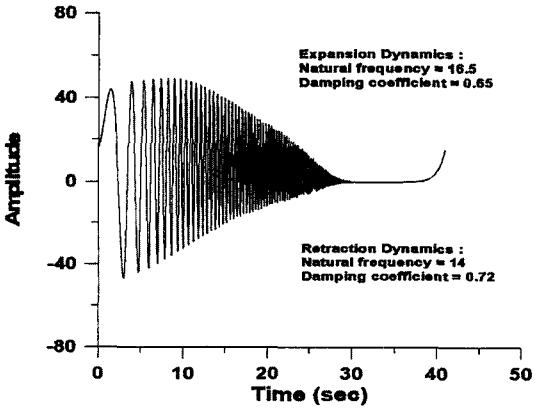

Fig. 4 Response of model 3 by the test signal

Table 1 The parameters to be estimated by the signal compression method with pre-processor (ω_n : natural frequency, ζ : damping coefficient)

Model No.	Characteristic	True values (ω_n, ζ)	Estimated values by the proposed method (ω_m, ζ)	Estimated values by SCM (ω_n, ζ)
1	expansion	14.0, 0.60	15.0, 0.60	13.8, 0.50
	retraction	14.0, 0.60	15.0, 0.60	
2	expansion	15.0, 0.58	16.0, 0.60	14.0, 0.55
	retraction	13.0, 0.66	13.5, 0.65	
3	expansion	16.5, 0.65	16.5, 0.60	14.6, 0.65
	retraction	14.0, 0.72	14.5, 0.70	

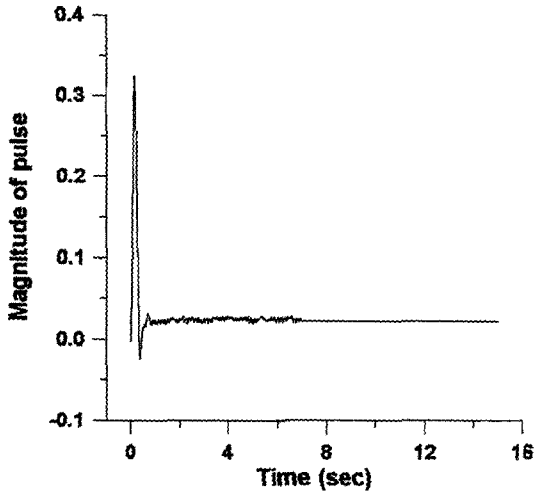

Fig. 5 Pulse response of expansion dynamics

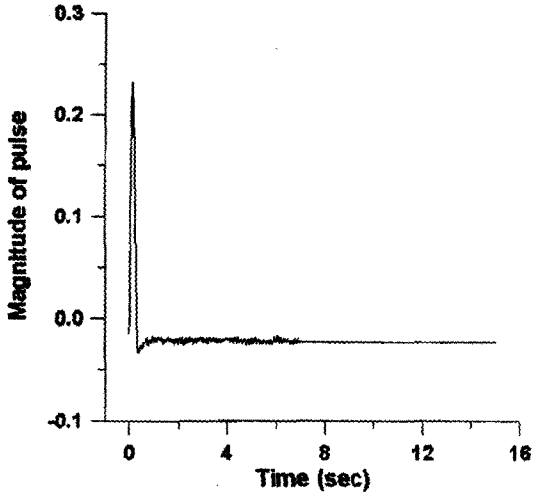

Fig. 6 Pulse response of retraction dynamics

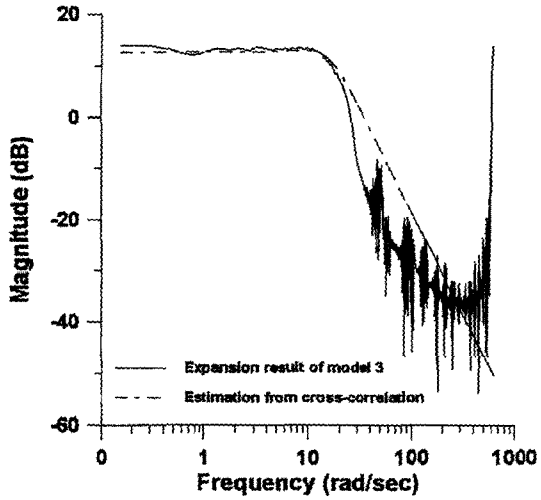

Fig. 7 Bode plot of expansion dynamics

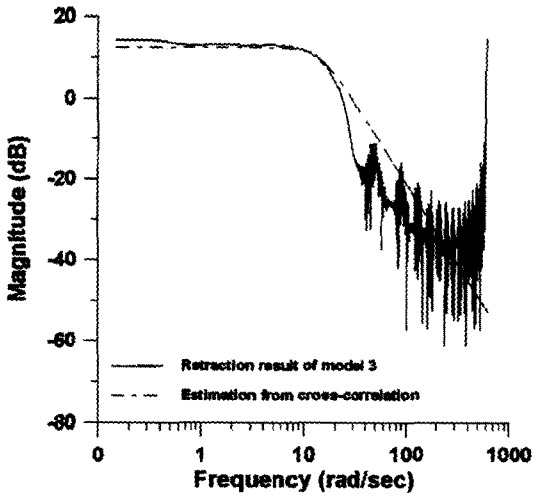

Fig. 8 Bode plot of retraction dynamics

signal compression process. The element contributed by the nonlinear component is also removed from the equivalent impulse response through a rectangular time window (0~7sec) as shown in Figs. 5 and 6. In this paper, the equivalent impulse response is called as the pulse response. By comparing the Bode plot of the model transfer function with the plot obtained from the pulse response of linear components, the natural frequency and damping coefficient are estimated as shown in Figs. 7 and 8. Bode plot of the pulse response from linear components and that of the estimated model are presented by a solid line and a dotted line, respectively, as shown in Figs. 7 and 8. The response of the model through the proposed method is very close to the response of the model 3 as shown in Fig. 4 and Fig. 9. However, the response of the model by the signal compression method without pre-processor is different from the that of the model 3 as shown in Fig. 10.

The unknown parameters are estimated by the proposed method. Table 1 shows the true values and the estimated values of the selected models. The performance of SCM is similar to that of SCM with pre-processor of which the parameters

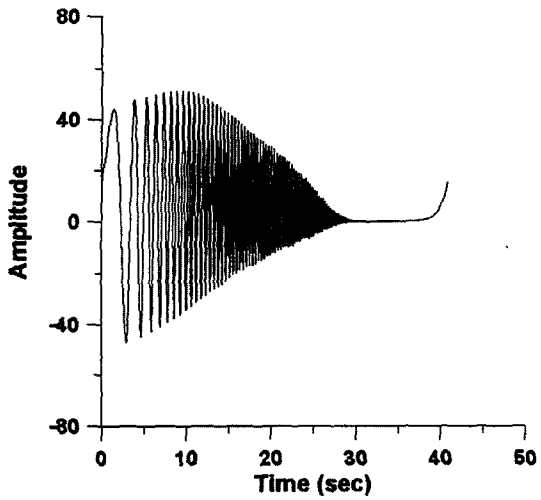

Fig. 9 Response of identified model by the SCM with pre-processor

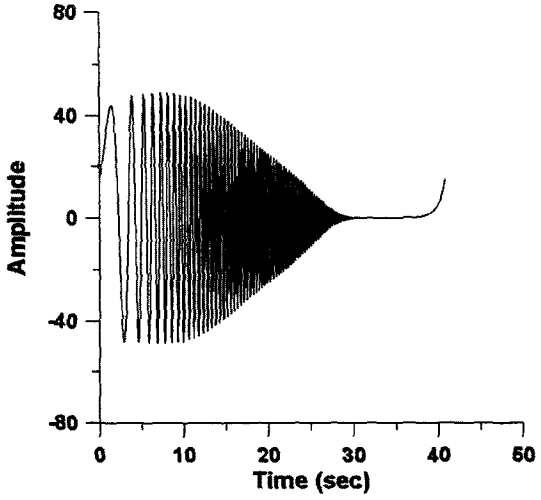

Fig. 10 Response of identified model by the SCM

related to the expansion and retraction are same (Model 1). However, in case of a unique system with two different dynamics according its motion (Model 2 and 3), the performance of the proposed method is much better than that of SCM as shown in Table 1. In case of Model 2, the estimated damping coefficient error by the proposed method is 0.02. However, that by the SCM is 0.11. Also, in case of Model 3, the estimated natural frequency error is 0.5, whereas that by the SCM is 1.9. Therefore, it is verified that the proposed method is valid for identifying a unique system with two dynamics.

3. Identification of Motion Platform

3.1 Modeling of stewart platform

The linear motions consist of longitudinal (surge), lateral (sway), and vertical (heave) motion. The angular motions are described by Bryant angles whose rotational sequences are x, y, and z axis. Here, q is set as the 6 DOF coordinate vector with surge (u), sway (v), heave (w), roll (α), pitch (β), and yaw (γ). This vector is presented by

$$q=[u,\ v,\ w,\ \alpha,\ \beta,\ \gamma]^T \tag{1}$$

Figure 11 shows the developed 6-DOF parallel motion platform with six single-rod cylinders and

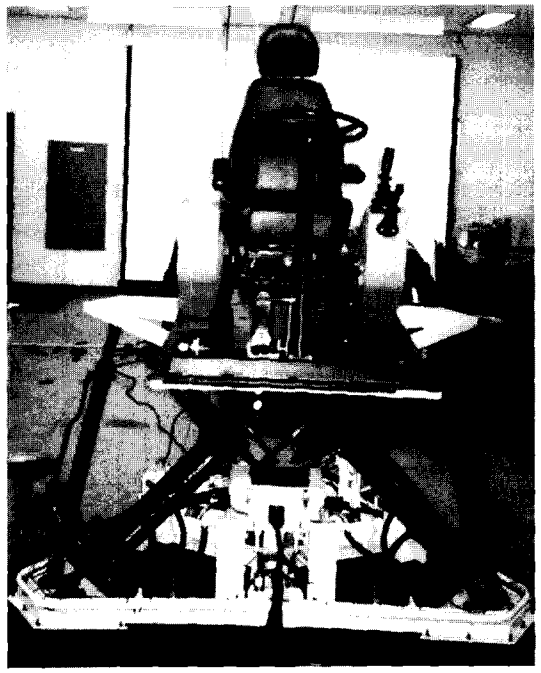

Fig. 11 Motion simulator with 6 single rod cylinders

the vehicle operating system (Lee et. al., 1999). Figure 12 shows the coordinates and notations of the Stewart platform. The coordinates are an inertial frame and the moving frame attached to the upper plate. The inertial frame $\{B\}(x_b,\ y_b,\ z_b)$ is fixed at the base plate, and the moving frame $\{P\}(x_p,\ y_p,\ z_p)$ at the upper plate. If the

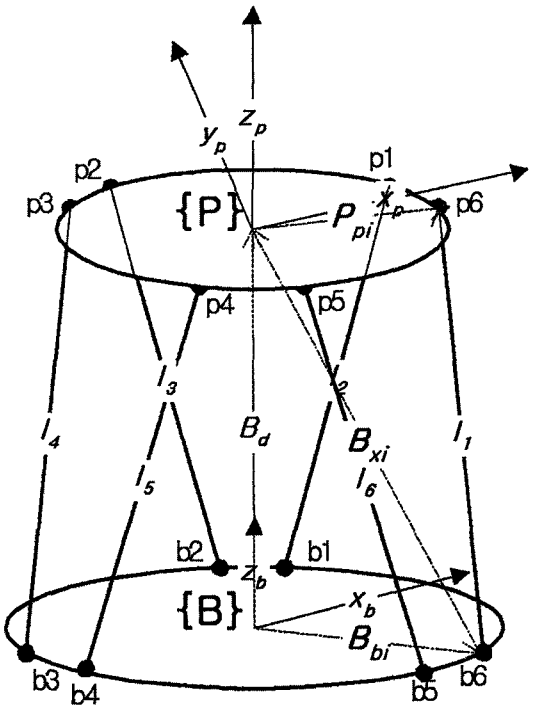

Fig. 12 Coordinate system of Stewart platform

rotational transformation matrix and the linear vector are presented by ${}^{P}_{B}R$ and B_d, respectively, the length vector (l_i) of the ith joint is written as

$$l_i = B_{qi} = B_d - B_{bi} + {}^{P}_{B}RP_{pi} \tag{2}$$

where,

$${}^{P}_{B}R = \begin{bmatrix} C_\beta C_\gamma & -S_\gamma C_\beta & C_\beta \\ C_\gamma S_\alpha S_\beta + C_\alpha S_\gamma & -S_\alpha S_\gamma S_\beta + C_\alpha C_\gamma & -S_\alpha C_\beta \\ -C_\gamma C_\alpha S_\beta + S_\alpha S_\gamma & C_\alpha S_\beta S_\gamma + S_\alpha C_\gamma & C_\alpha C_\beta \end{bmatrix}.$$

Thus, the cylinder lengths are computed by using the given position and orientation of the platform. This method is called the inverse kinematics of a Stewart platform. Solving the forward kinematic problem is not easy, because the solution of this problem can be analytically presented as the roots of 16-th or 40-th order polynomial, and not unique (Nair and Maddocks 1994). Therefore, numerical method such as the Newton-Rhapson method is widely used in order to solve the forward kinematics.

The dynamic equation of the Stewart platform considering all inertia effect is difficult to derive. Lebret derived the dynamic equation using the

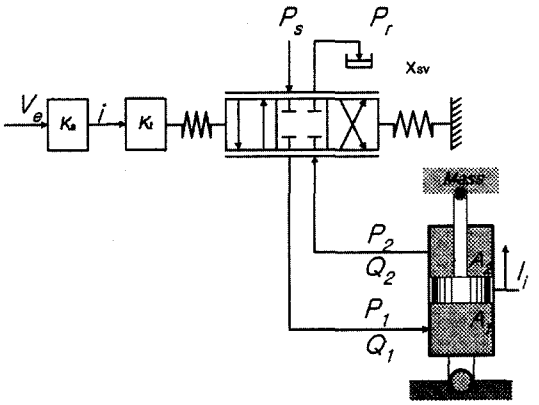

Fig. 13 Servovalve controlled single rod cylinder

Lagrange method and virtual work principle (Lebret et. al., 1993). This equation can be written as

$$M_P(q)\ddot{q} + C_P(q, \dot{q})\dot{q} + G_P(q) = J^T U_P \tag{3}$$

where, $M_P(q) \in R^{6\times6}$ is the inertia matrix, $C_P(q) \in R^{6\times6}$ corresponds to the centrifugal and Coriolis forces matrix, $G_P(q) \in R^{6\times1}$ is the gravity force vector, $J(q) \in R^{6\times6}$ is Jacobian matrix, and $U_P(q) \in R^{6\times1}$ is cylinder force vector. The detailed expressions of all terms of Eq. (3) are listed in the appendix. After algebraic operation such as $\dot{q} = J^{-1}\dot{l}$ and a kinematic transformation, Eq. (3) can be expressed as

$$\tilde{M}_P(q)\ddot{l} + \tilde{C}_P(q, \dot{q})\dot{l} + \tilde{C}_P(q) = U_P \tag{4}$$

where, $l = [l_1, l_2, l_3, l_4, l_5, l_6]^T$ is a vector of cylinder length,

$$\tilde{M}_P(q) = J^{-T}(q)M(q)J^{-1}(q)$$
$$\tilde{C}_P(q, \dot{q}) = J^{-T}(q)M(q)\frac{d}{dt}J^{-1}(q) + J^{-T}(q)C(q, \dot{q})J^{-1}(q)$$
$$\tilde{G}_P(q) = J^{-T}(q)G(q).$$

The dynamics of single-rod cylinder is considered. Figure 13 represents a servovalve controlled cylinder. Applying the generalized flow continuity equation and the linearlized flow equation of servovalve, an expanding dynamic equation and a retracting dynamic equation are expressed as

$$P_1=(K_1^e)^2R_0k_ix_{sv}-K_1^eR_0A_1\dot{l}+\frac{V_1}{\beta_e}\dot{P}_1$$
$$P_2=-(K_2^e)^2R_0k_ix_{sv}+K_2^eR_0A_2\dot{l}-\frac{V_2}{\beta_e}\dot{P}_2 \quad (5)$$

$$P_1=-(K_1^r)^2R_0k_ix_{sv}+K_1^rR_0A_1\dot{l}+\frac{V_1}{\beta_e}\dot{P}_1$$
$$P_2=(K_2^r)^2R_0k_ix_{sv}-K_2^rR_0A_2\dot{l}-\frac{V_2}{\beta_e}\dot{P}_2 \quad (6)$$

where, P_1 and P_2 are the pressure of each chamber, K_1^e, K_2^e, K_1^r, and K_2^r are the linearized coefficient constants for finite cylinder velocity, k_i and R_0 are flow gain and resistance, respectively. x_{sv} and β_e are the spool displacement and the effective bulk modulus of the fluid, respectively (Watton, 1989).

The effective bulk modulus of the fluid is much larger value than other constant parameters. Therefore the pressure variation terms of Eqs. (5) and (6) are negligible. So, these equations can be rewritten as

$$P_1=(K_1^e)^2R_0k_ix_{sv}-K_1^eR_0A_1\dot{l}$$
$$P_2=-(K_2^e)^2R_0k_ix_{sv}+K_2^eR_0A_2\dot{l} \quad (7)$$

$$P_1=-(K_1^r)^2R_0k_ix_{sv}+K_1^rR_0A_1\dot{l}$$
$$P_2=(K_2^r)^2R_0k_ix_{sv}-K_2^rR_0A_2\dot{l}. \quad (8)$$

Assuming the Stewart platform dynamics acts as an additional term to the cylinder model, the expanding and the retracting dynamics are obtained such as

$$M_A\ddot{l}+C_A\dot{l}+U_P=P_1A_1-P_2A_2 \quad (expansion)$$
$$=P_2A_2-P_1A_1 \quad (retraction) \quad (9)$$

where, M_A is the summation of equivalent masses of all the translational part of the cylinder, C_A is the equivalent damping coefficient, and U_P is defined as Eq. (4). Therefore, the nominal dynamic equation of the Stewart platform system including the manipulator and cylinder dynamics is obtained such as Eqs. (10) and (11) from Eqs. (4) and (9). The Eq. (10) is the expansion dynamics and the Eq. (11) is the retraction dynamics.

$$(\tilde{M}_P(q)+M_A)\ddot{l}+(\tilde{C}_P(q,\dot{q})+C_A+C_e)\dot{l}+\tilde{C}(q)=K_exsv \quad (10)$$

Table 2 Parameters of the servovalve controlled hydraulic cylinder

Parameter		Value
Servo Amp.	k_a	10 mA
Torque motor gain	k_t	0.000004064 m/mA
Cylinder Area	A_1	0.0013 m^2
	A_2	0.000641 m^2
Flow coefficient	K_{21}	0.8811
	K_{r1}	0.7462
Pressure coefficient	K_{e2}	0.4494
	K_{r2}	0.3806
Flow gain	k_i	23.44

$$(\tilde{M}_P(q)+M_A)\ddot{l}+(\tilde{C}_P(q,\dot{q})+C_A+C_r)\dot{l}+\tilde{C}(q)=K_rxsv \quad (11)$$

where, parameters are as follows:

$$K_2=(K_1^e)^2R_0K_iA_1+(K_2^e)^2R_0k_iA_2$$
$$C_e=K_1^eR_0(A_1)^2+K_2^eR_0(A_2)^2$$
$$K_r=(K_1^r)^2R_0k_iA_1+(K_2^r)^2R_0k_iA_2$$
$$C_r=K_1^rR_0(A_1)^2+K_2^rR_0(A_2)^2.$$

The relation of between input current of servovalve (i) and spool displacement (x_{sv}) is approximately expressed as

$$x_{sv}=k_ti \quad (12)$$

where, k_t is the torque motor gain of servovalve. And, the servovalve amplifier equation is also approximately written by

$$i=k_aV_e \quad (13)$$

where, k_a is a servo amplifier gain and V_e is an input voltage.

Therefore, the simplified dynamic equation of this system is rewritten by

$$M_T(q)\ddot{l}+C_E(q,\dot{q})\dot{l}+G_T(q)=K_eK_{sv}V_e \quad (14)$$
$$M_T(q)\ddot{l}+C_R(q,\dot{q})\dot{l}+G_T(q)=K_rK_{sv}V_e \quad (15)$$

where, $M_T=(\tilde{M}_P+M_A)$, $C_E=(\tilde{C}_P+C_A+C_e)$, $C_R=(\tilde{C}_P+C_A+C_r)$, $G_T=\tilde{G}_P(q)$, and $K_{sv}=k_tk_a$.

After separating the linear elements and the nonlinear elements from Eqs. (14) and Eq. (15),

these equations can be expressed as

$$M_{TL}\ddot{l}+C_{TL}\dot{l}+\Psi=KK_{SV}V_e \tag{16}$$

$$C_{TL}=\begin{cases} C_{EL} & \text{if expanding stroke} \\ C_{RL} & \text{if retraction stroke} \end{cases}$$

$$\Psi =\begin{cases} \Psi_E & \text{if expanding stroke} \\ \Psi_R & \text{if retraction stroke} \end{cases}$$

$$K =\begin{cases} K_e & \text{if expanding stroke} \\ K_r & \text{if retraction stroke} \end{cases}$$

where, M_{TL}, C_{EL}, and C_{RL} are the summation of all linear terms in M_T, C_E, and C_R, respectively. The perturbation terms Ψ_E and Ψ_R, which are the summation of the nonlinear terms and uncertainty terms among inertia moments, the Coriolis and centrifugal force, the gravity force, the friction force and the disturbance are expressed as

$$\Psi_{E,j}=\sum_{k=1,j\neq k}^{6}(M_T(j,k)\ddot{l}_k)+\sum_{k=1}^{6}(\Delta M_T(j,k)\ddot{l}_k) + \sum_{k=1,j\neq k}^{6}(C_E(j,k)\dot{l}_k)+\Delta C_{E,j}+G_j+\Delta G_j+d_j \tag{17}$$

$$\Psi_{R,j}=\sum_{k=1,j\neq k}^{6}(M_T(j,k)\ddot{l}_k)+\sum_{k=1}^{6}(\Delta M_T(j,k)\ddot{l}_k) + \sum_{k=1,j\neq k}^{6}(C_R(j,k)\dot{l}_k)+\Delta C_{R,j}+G_j+\Delta G_j+d_j \tag{18}$$

where, 'Δ' is the uncertainty term and d_j is the disturbance term.

3.2 Estimation of uncertain parameters

To estimate the uncertain parameters (M_{TL} and C_{TL}) of the motion platform in Eq. (16), the test signal in Fig. 1 is supplied through the D/A converter. The length of the cylinder moving according to the supplied test signal is detected by linear differential transducer and A/D converter. The output signal is shown in Fig. 14. It is shown that the dynamic properties in expansion and retraction motion are different from each other. To identify the system dynamics, the signal is separated in the expansion and retraction motion such as shown in simulation. The separated ex-

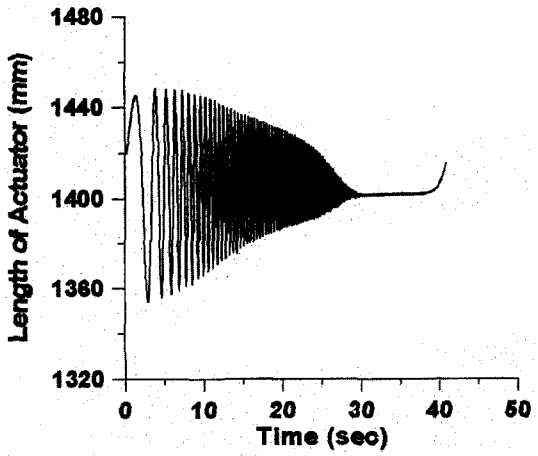

Fig. 14 Response from the cylinder by the test signal

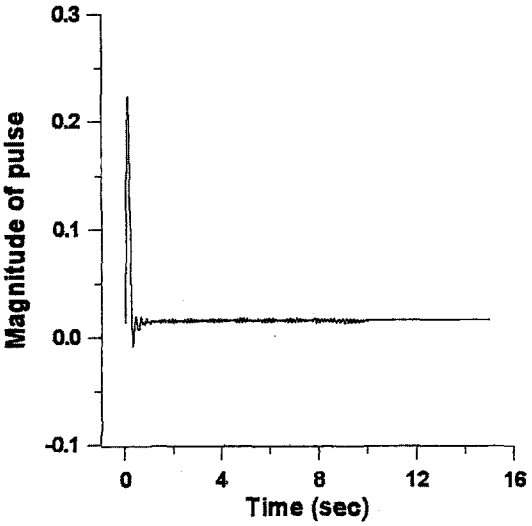

Fig. 15 Pulse response of expansion

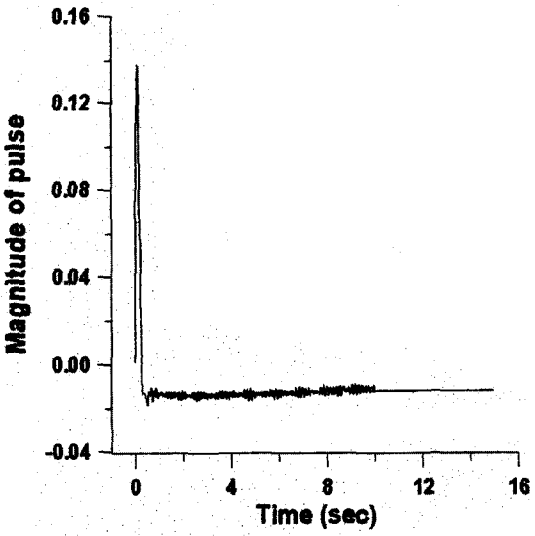

Fig. 16 Pulse response of retraction

pansion and retraction signals are changed into pulse responses through the signal compression process which consists of the FFT algorithm, the mathematical inverse phase-shift filter in the frequency domain, and IFFT. The element contributed by the nonlinear component is removed from the pulse response. Figures 15 and 16 show each pulse response from the expansion motion and the retraction one, respectively. By comparing Bode plot of the transfer function from a model with that obtained from the pulse response, natural frequency (ω_n) and damping coefficient (ζ) are estimated as shown in Figs. 17 and 18. As these processes are applied to all of the cylinders of the motion platform, the natural frequency and damping coefficient of each cylinder are obtained. Therefore, uncertain parameters (M_{TL} and C_{TL}) of Eq. (16) are obtained by the natural frequency and the damping coefficient. The linear close-loop system of the motion platform is expressed as

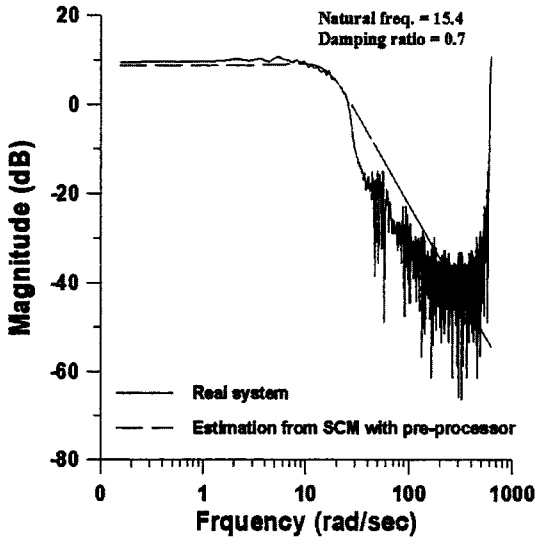

Fig. 17 Bode plot of expansion

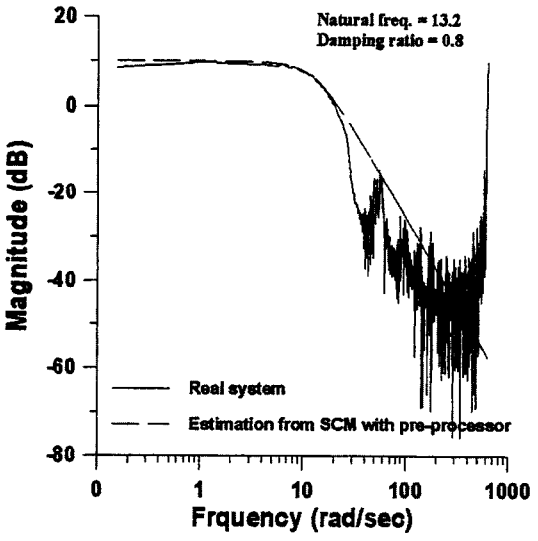

Fig. 18 Bode plot of retraction

$$G_C=\frac{L(S)}{V_e(s)}=\frac{K_pK_{sv}K}{M_{TL}S^2+C_{TL}S+K_pK_{sv}K}. \quad (19)$$

And, the linear close-loop system of the general mass-damper system is defined as

$$G_C=\frac{\omega_n^2}{S^2+2\zeta\omega_nS+\omega_n^2}. \quad (20)$$

So, the equivalent mass and damping coefficient of each cylinder is calculated as

$$M_{TL}=\frac{K_pK_{sv}K}{\omega_n^2},\ C_{TL}=2\zeta\sqrt{K_pK_{sv}KM_{TL}} \quad (21)$$

where, K_P is proportional control gain.

Table 3 shows the estimated equivalent mass and damping coefficient of each cylinder.

Table 3 Estimation result for the motion platform

Cylinder No.	Direction	ω_n, ζ	M_{TL}(kg), C_{TL}(kg/s)
1	expansion	15.4, 0.7	92.6, 1997. 2
	retraction	13.2, 0.8	90.4, 1909. 9
2	expansion	15.2, 0.7	95.1, 2032. 5
	retraction	13.0, 0.8	93.2, 1939. 3
3	expansion	15.2, 0.7	95.1, 2032. 5
	retraction	13.2, 0.8	90.4, 1909. 9
4	expansion	15.4, 0.7	92.6, 1997. 2
	retraction	13.4, 0.8	87.8, 1881. 4
5	expansion	15.6, 0.7	90.2, 1971. 6
	retraction	13.4, 0.8	87.8, 1881. 4
6	expansion	15.2, 0.7	95.1, 2032. 5
	retraction	13.0, 0.8	93.2, 1939. 3

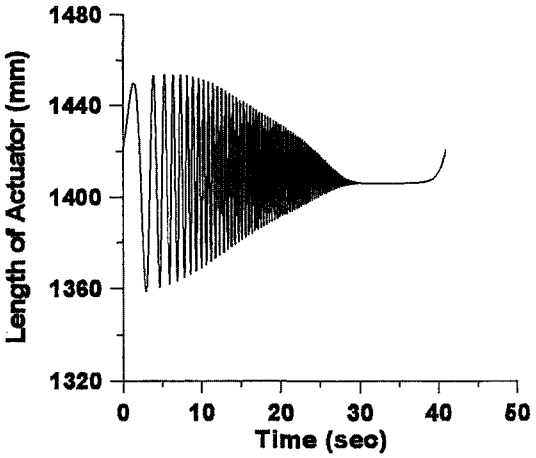

Fig. 19 Response from the identified model by the SCM with pre-processor

Figure 19 shows the output result from the identified model when the test signal is supplied to the model. It is shown that the output signal from the identified model in Fig. 19 is similar to that from the real system in Fig. 14. Therefore it is verified that the proposed method can be used for estimation of the unknown parameters even though the system has two different dynamics.

4. Application to Sliding Mode Control

4.1 Design of sliding mode controller in joint-axis

A real-time control system was developed for position control of the Stewart platform. The schematic diagram of the control system is shown in Fig. 20. The control board is composed of a microprocessor and peripheral circuits with a DIO (digital input and output), an ADC (analog to digital converter), a DAC (digital to analog converter), a serial communication circuit and timers as shown in Fig. 21. The micro-processor of the control board is 80C196KC. For improving computational ability, one micro-processor controls two cylinders. Hence, the motion controller is composed of three control boards. The dynamic system regarding nonlinear terms such as disturbance and perturbation can be represented by Eq. (16). The parameters of this equation were estimated by the proposed signal compression

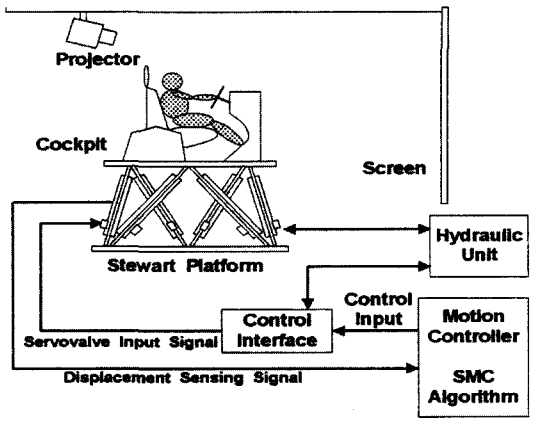

Fig. 20 Block diagram of control system

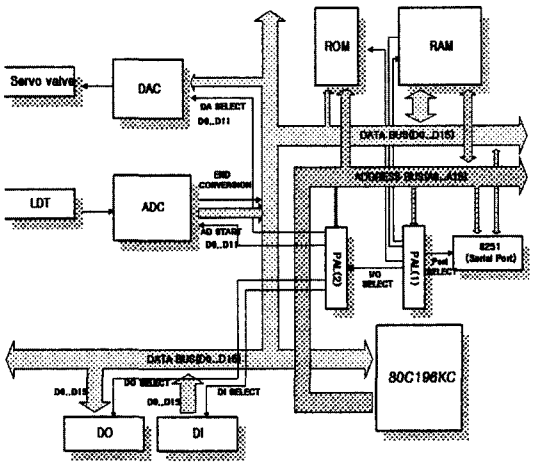

Fig. 21 Schematic diagram of motion control board based on 80C196KC

method with pre-processor.

The hydraulic motion platform is a complex nonlinear system. Therefore, a control performance is not so good by using a classical control algorithm such as PID controller. Sliding mode control is very attractive method for nonlinear systems. It has been confirmed as a control approach for nonlinear systems being robust against parameters and load variations. Therefore, sliding mode controller is designed and applied to the hydraulic motion platform. Let the desired length, velocity, and acceleration of the i-th cylinder be denoted by $l_{d,j}$, $\dot{l}_{d,j}$, and $\ddot{l}_{d,j}$ respectively, and the corresponding measured quantities denoted by l_j, $\dot{l}_j$, and $\ddot{l}_j$ respectively. The errors are defined as

$$e_j=l_j-l_{d,j},\ \dot{e}_j=\dot{l}_j-\dot{l}_{d,j},\ \text{and}\ \ddot{e}_j=\ddot{l}_j-\ddot{l}_{d,j} \quad (22)$$

The sliding surface (s_j) is defined as

$$s_j=\dot{e}_j+c_je_j \qquad j=1,\ 2,\ \cdots,\ 6 \quad (23)$$

where the positive constant c_j is the desired control bandwidth. Let the time derivative of the Lyapunov function candidate be given by $s\dot{s}<0$ to satisfy the boundary layer attraction condition. When the unmodeled nonlinear terms are replaced by disturbances, a control input (Lee et. al., 1998) is proposed as

$$U_A=u_j=\psi_{\alpha i}e_j+\psi_{fj}+\psi_{\beta i}\dot{l}_{dj}+\psi_{\gamma i}\ddot{l}_{dj} \quad (24)$$

$$\psi_{\alpha j}=\begin{cases}\alpha_{1j} & \text{if } s_je_j>0\\ \alpha_{2j} & \text{if } s_je_j<0\end{cases}$$

$$\psi_{\beta j}=\begin{cases}\beta_{1j} & \text{if } s_j\dot{l}_{dj}>0\\ \beta_{2j} & \text{if } s_j\dot{l}_{dj}<0\end{cases}$$

$$\psi_{\gamma j}=\begin{cases}\gamma_{1j} & \text{if } s_j\ddot{l}_{dj}>0\\ \gamma_{2j} & \text{if } s_j\ddot{l}_{dj}<0\end{cases}$$

$$\psi_{fj}=\begin{cases}u_{fj}^-=M_{1j}+M_{2j}\times|\,e_j\,| & \text{if } s_j>0\\ u_{fj}^+=-M_{1j}-M_{2j}\times|\,e_j\,| & \text{if } s_j<0\end{cases}$$

where $\psi_{\beta i}$ and $\psi_{\gamma i}$ are each feedforward control input term to satisfy the existence condition of sliding mode against unfavorable effects of $\dot{l}_{di}$ and $\ddot{l}_{di}$ on the trajectory tracking, respectively. ψ_{fi} is the modified control input for compensating disturbances.

From Eqs. (16) and (24), the existence condition of the sliding mode can be derived as

$$\begin{aligned}s_j\dot{s}_j&=s_j(c_j\dot{e}_j+\ddot{e}_j)\\&=s_j^2\left(c_j-\frac{C_{TL,j}}{M_{TL,j}}\right)+s_je_j\left(\frac{C_{TL,j}}{M_{TL,j}}c_j+\frac{KK_{SV,j}}{M_{TL,j}}\psi_{\alpha j}-c_j^2\right)\\&\quad+\left(\frac{KK_{SV,j}}{M_{TL,j}}\psi_{fj}-\frac{\Psi_j}{M_{TL,j}}\right)s_j+\left(\frac{KK_{SV,j}}{M_{TL,j}}\psi_{\beta j}-\frac{C_{TL,j}}{M_{TL,j}}\right)s_j\dot{l}_{d,j}\\&\quad+\left(\frac{KK_{SV,j}}{M_{TL,j}}\psi_{\gamma i}-1\right)s_j\ddot{l}_{d,j}<0.\end{aligned} \quad (25)$$

If all terms in Eq. (25) are negative, the existence condition of sliding mode is always satisfied. And, Eq. (25) can be used to obtain the limit values of all the switching parameters in Eq. (24). When the first term in Eq. (25) is negative ($c_j<C_{TL,j}/M_{TL,j}$), the limit values of the switching parameters can be derived as follows:

$$\begin{cases}KK_{SV,j}\alpha_{1j}+C_{TL,j}c_j-M_{TL,j}c_j^2<0 & \text{if } s_je_j>0\\ KK_{SV,j}\alpha_{2j}+C_{TL,j}c_j-M_{TL,j}c_j^2>0 & \text{if } s_je_j<0\end{cases}$$

$$\begin{cases}u_{fj}^-=\ M_{1,j}+M_{2,j}\,|\,e_i\,|<\Psi_j/KK_{SV,j} & \text{if } s_j>0\\ u_{fj}^+=-M_{1,j}-M_{2,j}\,|\,e_i\,|<\Psi_j/KK_{SV,j} & \text{if } s_j<0\end{cases}$$

$$\begin{cases}KK_{SV,j}\beta_{1j}-C_{TL,j}<0 & \text{if } s_j\dot{l}_{dj}>0\\ KK_{SV,j}\beta_{2j}-C_{TL,j}>0 & \text{if } s_j\dot{l}_{dj}<0\end{cases}$$

$$\begin{cases}KK_{SV,j}\gamma_{1j}-M_{TL,j}<0 & \text{if } s_j\ddot{l}_{dj}>0\\ KK_{SV,j}\gamma_{2j}-M_{TL,j}>0 & \text{if } s_j\ddot{l}_{dj}<0\end{cases}$$

The magnitude of the nonlinear terms in Eqs. (17) and (18) is assumed to decrease as the error converges to zero. Therefore, the value of $M_{2,j}$ in ψ_{fi} is proportional to the absolute value of the error influencing the chattering magnitude. That is, ψ_{fi} can be smaller because the magnitude of nonlinear terms related to the tracking error is smaller as the trajectory converges to a desired trajectory. Therefore, the smaller supplied ψ_{fi} reduces chattering. The value of $M_{1,j}$ in ψ_{fi} is selected based on the maximum value of Ψ.

4.2 Experiment

A simple tracking control is performed to check the identified model and sliding mode control algorithm. To determine the switching control parameters, the values of M_{TL} and C_{TL} of the whole system are obtained experimentally using the signal compression method with pre-processor as shown in the Table 3. The limit values of the switching parameters which are satisfied the existence condition of sliding mode are derived by using the identified parameters and $c_j=20$, and they are listed in Table 4.

The tuned control parameters c_j, $\psi_{\alpha,j}$, $\psi_{\beta,j}$, $\psi_{\gamma,j}$ from boundary conditions to satisfy sliding mode are selected as shown in the Table 5. $M_{1,j}$ and $M_{2,j}$ are selected as -10 and -2 by trial and error method, respectively. The payload of the system is about 250 kg. The sampling time interval for control is selected as 10 msec because the response frequency of servovalve is 100 Hz.

The reference trajectories and tracking trajectories are shown in Fig. 22. Figsures 23~25 show tracking position errors of cylinder 1, 3, and 6,

Table 4 Limit values of switching parameters by using the signal compression method

Cylinder No.	Stroke	c_j	$\alpha_j(c_j=20)$	$\beta_j(c_j=20)$	$\gamma_j(c_j=20)$
Cylinder #1	Expansion	$c_1<21.6$	$\alpha_{11}<-3.2889$ $\alpha_{21}>-3.2889$	$\beta_{12}<2.2727$ $\beta_{21}>2.2727$	$\gamma_{11}<0.1054$ $\gamma_{21}>0.1054$
	Retraction	$c_1<21.1$	$\alpha_{11}<-3.2140$ $\alpha_{21}>-3.2140$	$\beta_{11}<3.0303$ $\beta_{21}>3.0303$	$\gamma_{11}<0.1435$ $\gamma_{21}>0.1435$
Cylinder #2	Expansion	$c_2<21.3$	$\alpha_{12}<-2.7701$ $\alpha_{22}>-2.7701$	$\beta_{12}<2.3026$ $\beta_{22}>2.3026$	$\gamma_{12}<0.1082$ $\gamma_{22}>0.1082$
	Retraction	$c_2<20.8$	$\alpha_{12}<-2.3669$ $\alpha_{22}>-2.3669$	$\beta_{12}<3.0769$ $\beta_{22}>3.0769$	$\gamma_{12}<0.1479$ $\gamma_{22}>0.1479$
Cylinder #3	Expansion	$c_3<21.3$	$\alpha_{13}<-2.7701$ $\alpha_{23}>-2.7701$	$\beta_{13}<2.3026$ $\beta_{23}>2.3026$	$\gamma_{13}<0.1082$ $\gamma_{23}>0.1082$
	Retraction	$c_3<21.1$	$\alpha_{13}<-3.2140$ $\alpha_{23}>-3.2140$	$\beta_{13}<3.0303$ $\beta_{23}>3.0303$	$\gamma_{13}<0.1435$ $\gamma_{23}>0.1435$
Cylinder #4	Expansion	$c_4<21.6$	$\alpha_{14}<-3.2889$ $\alpha_{24}>-3.2889$	$\beta_{14}<2.2727$ $\beta_{24}>2.2727$	$\gamma_{14}<0.1054$ $\gamma_{24}>0.1054$
	Retraction	$c_4<1.4$	$\alpha_{14}<-4.0098$ $\alpha_{24}>-4.0098$	$\beta_{14}<2.9851$ $\beta_{24}>2.9851$	$\gamma_{14}<0.1392$ $\gamma_{24}>0.1392$
Cylinder #5	Expansion	$c_5<21.9$	$\alpha_{15}<-3.7804$ $\alpha_{25}>-3.7804$	$\beta_{15}<2.2436$ $\beta_{25}>2.2436$	$\gamma_{15}<0.1027$ $\gamma_{25}>0.1027$
	Retraction	$c_5<21.4$	$\alpha_{15}<-4.0098$ $\alpha_{25}>-4.0098$	$\beta_{15}<2.9851$ $\beta_{25}>2.9851$	$\gamma_{15}<0.1392$ $\gamma_{25}>0.1392$
Cylinder #6	Expansion	$c_2<21.3$	$\alpha_{16}<-2.7701$ $\alpha_{26}>-2.7701$	$\beta_{16}<2.3026$ $\beta_{26}>2.3026$	$\gamma_{16}<0.1082$ $\gamma_{26}>0.1082$
	Retraction	$c_2<20.8$	$\alpha_{16}<-2.3669$ $\alpha_{26}>-2.3669$	$\beta_{16}<3.0769$ $\beta_{26}>3.0769$	$\gamma_{16}<0.1479$ $\gamma_{26}>0.1479$

Table 5 Tuned control parameter of sliding mode control

Parameter / Cylinder no.	α_j	β_j	γ_j
Cylinder #1	$\alpha_{11}=-25$ $\alpha_{21}=17$	$\beta_{11}=-1.5$ $\beta_{21}=3.0$	$\gamma_{11}=-0.2$ $\gamma_{21}=0.2$
Cylinder #2	$\alpha_{12}=-27$ $\alpha_{22}=20$	$\beta_{12}=-2.0$ $\beta_{22}=4.0$	$\gamma_{12}=-0.2$ $\gamma_{22}=0.2$
Cylinder #3	$\alpha_{13}=-27$ $\alpha_{23}=17$	$\beta_{13}=-2.0$ $\beta_{23}=4.0$	$\gamma_{13}=-0.2$ $\gamma_{23}=0.2$
Cylinder #4	$\alpha_{14}=-22$ $\alpha_{24}=17$	$\beta_{14}=-1.5$ $\beta_{24}=3.0$	$\gamma_{14}=-0.2$ $\gamma_{24}=0.2$
Cylinder #5	$\alpha_{15}=-25$ $\alpha_{25}=20$	$\beta_{15}=-1.5$ $\beta_{25}=3.0$	$\gamma_{15}=-0.2$ $\gamma_{25}=0.2$
Cylinder #6	$\alpha_{16}=-27$ $\alpha_{26}=20$	$\beta_{16}=-2.0$ $\beta_{26}=4.0$	$\gamma_{16}=-0.2$ $\gamma_{26}=0.2$

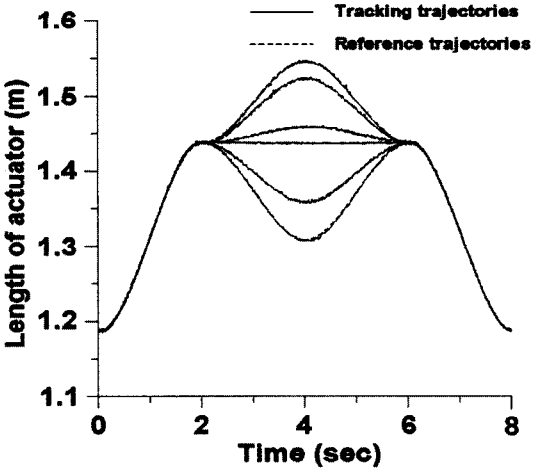

Fig. 22 Reference trajectories and tracking trajectories

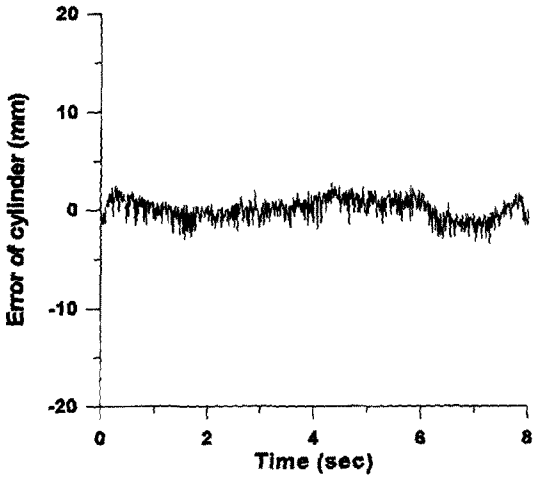

Fig. 23 Tracking error of cylinder 1

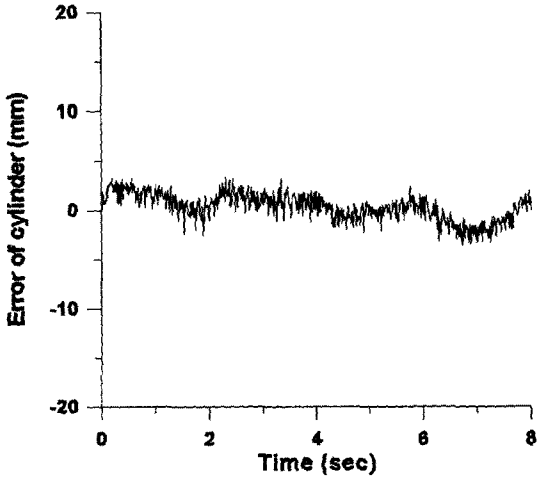

Fig. 25 Tracking error of cylinder 6

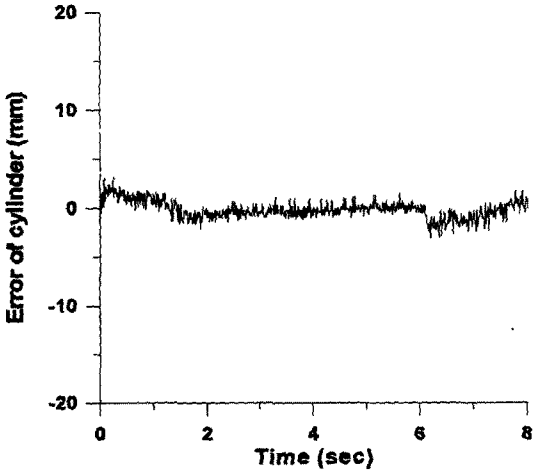

Fig. 24 Tracking error of cylinder 3

respectively. In fast motion for z-axis, maximum error is about 4 mm. However, average error for the whole of motion is within 2.5 mm. That is, the tracking performance of the designed sliding mode control is relatively good. It shows that the estimated parameters was useful to get the control parameters c_j, $\psi_{\alpha,j}$, $\psi_{\beta,j}$, $\psi_{\gamma,j}$.

5. Conclusion

It is difficult to analyze and identify a system with the two different dynamic properties such as a single-rod cylinder by using general estimation method, because of non-linearity caused by the difference of each chamber volume.

This paper proposed a new identification method which is able to estimates uncertain parameters of this system as separating two different dynamic properties by the signal compression method with pre-processor. It is shown that the estimated values obtained by the proposed method are very close to the true values by the simulation and the experiment as shown in the results. The performance of SCM is similar to that of SCM with pre-processor in which the parameters related to the expansion and retraction are same (Model 1). However, In case of a unique system with two different dynamics according its motion, the performance of the proposed method is absolutely better than that of SCM as shown in Table 1. In case of Model 2, the estimated damping coefficient error by the proposed method is 0.02. However, that by the SCM is 0.11. Also, in case of Model 3, the estimated natural frequency error is 0.5, whereas that by the SCM is 1.9. Therefore, it is verified that the proposed method is valid for identifying a unique system with two dynamics.

As its application, a sliding mode controller was designed on the basis of the identified model for the Stewart platform and evaluated experimentally. The tracking performance of the designed sliding mode control was relatively good. Therefore, it was proved that the identified model

for the Stewart platform by the proposed method is useful to design the sliding mode controller.

Acknowledgment

This research was supported by the KOSEF (Korea Science and Engineering Foundation, basic research grants : 97-02-00-10-01-5), and partially by the Brain Korea 21 project and the Science Research Fund of School of Mechanical Engineering, Pusan National University.

References

Hashimoto, H., Maruyama, K. and Harashima, F., 1987, "A Microprocessor-Based Robot Manipulator Control with Sliding Mode," *IEEE Trans. Industrial Electronics*, Vol. 34, No. 1, pp. 11～18.

Lee, M. C. and Aoshima, N., 1989, "Identification and Its Evaluation of the System with a Nonlinear Element by Signal Compression Method," *Trans. of SICE*, Vol. 25, No. 7, pp. 729～736.

Lee, M. C., Park, M. K., Son, K., Yoo, W. S. and Han, M. C., 1999, "The Development of a Driving Simulator for Reappearance of a Vehicle Motion," *Proc. of the 1999 ICMT*, pp. 589～594.

Lee, M. C., Son, K. and Lee, J. M., 1998, "Improving Tracking Performance of Industrial SCARA Robots Using a New Sliding Mode Control Algorithm," *KSME International Journal*, Vol. 12, No. 5 pp. 761～772.

Lebret, G., Liu, K. and Lewis, F. L., 1993, "Dynamic Analysis and Control of a Stewart Platform Manipulator," *Journal of Robotic Systems*, Vol. 10, No. 5, pp. 629～655.

Masui, G., Nishikawa, K. and Kiya, H., 2000, "2D Blind System Identification Using Adaptive Algorithm," *Proc. of the 2000 TENCON*, Vol. 2, pp. 77～79a.

Nair, R. and Maddocks, J., 1994, "On the Forward Kinematics of Parallel Manipulators," *International Journal of Robotics Research*, Vol. 13, No. 2, pp. 171～188.

Slotine, J. J., 1985, "The Robust Control of Robot Manipulators," *Int. J. of Robotics Research*, Vol. 4, No. 4, pp. 49～64.

Stewart, D., 1966, "A Platform with Six Degree of Freedom," *Proc. of the Institute of Mechanical Engineering*, Vol. 180, pp. 317～386.

Watton, J., 1989, *Fluid Power Systems : Modeling, Simulation, Analog and Microcomputer Control*, Prentice Hall, pp. 95～116.

Widrow, B. and Stearns, S. D., 1985, *Adaptive Signal Processing*, Prentice-Hall, p. 195.

Yang, S. Y., Lee, M. C., Lee, M. H. and Arimoto, S., 1998, "Measuring System for Development of Stroke-Sensing Cylinder for Automatic Excavator," *IEEE Trans. on Industrial Electronics*, Vol. 45, No. 3, pp. 376～384.

Zou, Y. and Chan, S. C., 1999, "A Robust M-estimate Adaptive Filter for Impulse Noise Suppression," *Proc. of 1999 Int. Conf. on Acoustics, Speech, and Signal Processing*, Vol. 4, pp. 1765～1768.

Appendix

$$M_P=\begin{bmatrix} m_u & 0 & 0 & 0 & 0 \\ 0 & m_u & 0 & 0 & 0 \\ 0 & 0 & m_u & 0 & 0 \\ 0 & 0 & 0 & M_{45} & M_{46} \\ 0 & 0 & 0 & M_{55} & M_{56} \\ 0 & 0 & 0 & M_{65} & M_{66} \end{bmatrix}$$

$$M_{44}=C_\beta(I_xC_\gamma^2+I_yS_\gamma^2)+I_zS_\beta^2$$

$$M_{45}=M_{54}=(I_x-I_y)\,C_\gamma S_\gamma C_\beta$$

$$M_{46}=M_{64}=I_zS_\beta$$

$$M_{55}=I_xS_\gamma^2+I_yC_\gamma^2$$

$$M_{56}=M_{65}=0$$

$$M_{66}=I_z$$

$$C_P=\begin{bmatrix} 0 & 0 & 0 & 0 & 0 & 0 \\ 0 & 0 & 0 & 0 & 0 & 0 \\ 0 & 0 & 0 & 0 & 0 & 0 \\ 0 & 0 & 0 & C_{44} & C_{45} & C_{46} \\ 0 & 0 & 0 & C_{54} & C_{55} & C_{56} \\ 0 & 0 & 0 & C_{64} & C_{65} & C_{66} \end{bmatrix}$$

$$C_{44}=-k_1\dot{\beta}-k_2\dot{\gamma}$$
$$C_{45}=-k_1\dot{\alpha}-k_3\dot{\beta}+(k_4+k_5)\,\dot{\gamma}$$
$$C_{46}=-k_2\dot{\alpha}+(k_5+k_4)\,\dot{\beta}$$
$$C_{54}=k_1\dot{\alpha}+(k_4-k_5)\,\dot{\gamma}$$
$$C_{55}=k_5\dot{\gamma}$$
$$C_{56}=(k_4-k_5)\,\dot{\alpha}+k_6\dot{\beta}$$
$$C_{64}=k_2\dot{\alpha}+(k_5-k_4)\,\dot{\beta}$$
$$C_{65}=(k_5-k_4)\,\dot{\alpha}-k_6\dot{\beta}$$
$$C_{66}=0$$

$$k_1=C_\beta S_\beta(C_\gamma^2 I_x+S_\gamma^2 I_y-I_z)$$
$$k_2=C_\beta^2 C_\gamma S_\gamma(I_x-I_y)$$
$$k_3=C_\gamma S_\gamma S_\beta(I_x-I_y)$$
$$k_4=\frac{1}{2}[C_\beta(C_\gamma^2-S_\gamma^2)\,(I_x-I_y)]$$
$$k_5=\frac{1}{2}I_z C_\beta$$
$$k_6=C_\gamma S_\gamma(I_x-I_y)$$

$$G_{P=}[0\ 0\ m_u g\ 0\ 0\ 0]^T$$